JARQ 60 (1), 19-32 (2026) https://www.jircas.go.jp

Mineralogical and Chemical Properties of Low-Grade African Phosphate Rocks for Agricultural Applications

Toshio IMAI[1], Takashi KANDA[2], Jacques SAWADOGO[3], Fujio NAGUMO[4] and Satoshi NAKAMURA[4]*

[1] Central Research Laboratory, Taiheiyo Cement Corporation, Sakura, Japan
[2] Tropical Agriculture Research Front (TARF), Japan International Research Center for Agricultural Sciences (JIRCAS), Ishigaki, Japan
[3] Institut de l'Environnement et de Recherches Agricoles (INERA), Kamboinse, Ouagadougou, Burkina Faso
[4] Japan International Research Center for Agricultural Sciences (JIRCAS), Tsukuba, Japan

Abstract

Although sub-Saharan African countries comprise a large amount of low-grade phosphate rock (PR), they do not consume this because of the high cost of P fertilizer processing. For less expensive P fertilizers, a suitable processing method must be selected for each low-grade PR. As phosphate solubility and suitable processing differ by PR, ten low-grade African PRs were collected from different countries and analyzed. Their phosphate solubilities correlated with their chemical and mineralogical compositions. Based on mineral composition-related results supported by TG-DTA and XRD analyses, we broadly classified the ten low-grade African PRs into five groups. These low-grade PRs consisted mainly of hydroxyapatite and were suitable for direct application to agricultural land as powdered PR. Low-grade PRs with low Fe and Al contents are suitable for partial acidulation and may be effective, whereas low-grade PRs with high Fe, Al, and heavy metal contents are suitable for high-temperature treatment. Regardless of the difference in origin, the phosphate solubility of low-grade African PRs is indicated by 2% citric acid solubility, assuming a dependence on the crystallite sizes of francolite and fluorapatite.

Discipline: Agricultural Environment
Additional key words: crystallinity, fluorapatite, francolite, full width at half maximum, solubility

Introduction

Phosphorus (P) is an essential element for crop production. However, approximately 30% of the global agricultural land is P-deficient (MacDonald et al. 2011). Soil P fertility is primarily determined by the amount applied to and retained by the soil, with highly weathered soils in tropical regions, such as Africa, having particularly high P retention (Nishigaki et al. 2021). However, due to the low levels of P application in sub-Saharan Africa, the soil-available phosphorous content is generally low, limiting crop production in the region (Saito et al. 2019). Adequate fertilizer application is necessary to improve crop yields in sub-Saharan Africa, but extremely high fertilizer prices have prevented its widespread adoption. Inexpensive P resources accessible to small-scale farmers must be provided to overcome this.

Phosphate deposits exist in many sub-Saharan African countries, with estimated reserves of 16.7 billion tons (Van Kauwenbergh 2010). However, these deposits exist predominantly as low-grade phosphate rocks (PRs), which have low phosphate content and solubility, resulting in their underutilization (Nakamura et al. 2013, Appleton 2002). However, if low-grade PRs could be utilized as affordable P resources, the low-P soil environment in the region would be enriched, thereby improving crop productivity.

Low-grade PRs are generally difficult to convert into fertilizers and are usually applied directly to

*Corresponding author: nakamuras0203@jircas.go.jp
Received 7 November 2024; accepted 15 April 2025; J-STAGE Advanced Epub 20 October 2025.
https://doi.org/10.6090/jarq.24J17

agricultural land as PR powder. However, their application effectiveness varies with factors such as PR solubility, soil environment, crop, and climatic environment (Chien & Menon 1995). Low-solubility PRs are slow-acting and require a prolonged time for their effects to manifest. Their effects were reported to be severely limited in high-P-absorbing soil environments (Fukuda et al. 2013). Therefore, to ensure that the phosphate component of low-grade PRs functions effectively as a fertilizer, modification strategies that involve enhancing the water-soluble P content are imperative.

Physical, biological, and chemical solubilization methods were developed to improve phosphate solubility of low-grade PRs (Nakamura et al. 2013). Physical methods, such as reducing the particle size to the nanoscale and increasing the total surface area, can enhance the efficiency of low-grade PR, making it a more effective phosphorus fertilizer (Abd El-Halim & Omae 2019, Liu & Lal 2015). Phospho-composting is a traditional biological solubilization method for low-grade PRs and has demonstrated high effectiveness in its application (Chtouki et al. 2022, Sagnon et al. 2022). Solid-state fermentation (SSF) using oxalic acid and *Aspergillus niger* was investigated as a promising approach (Rodrigues et al. 2024). The chemical treatment of partial acidulation involves treating low-grade PRs with a specific quantity of acid to fully convert insoluble phosphate minerals into water-soluble monocalcium phosphate monohydrate (Hammond et al. 1986). Partially acidulated phosphate rocks (PAPRs) have higher water and citric acid (CA) solubilities than raw powders, and their effectiveness has been evaluated in West African countries (Adediran & Sobulo 1998, Sedogo et al. 1991). However, the phosphate solubility of PAPRs depends on the origin of the low-grade PRs. In particular, the high levels of Fe, Al, and Si impurities prevent their conversion into fertilizers. Hammond et al. (1989) found that the solubility of the phosphate component of PAPRs containing low-grade PRs with high levels of Fe and Al was low.

Heat treatment methods, such as fusing and calcining phosphate fertilizers, are another effective method applicable to low-grade PRs. Akiyama (1988) increased phosphate solubility by calcining low-grade PR containing large amounts of Fe, Al, and Si with calcium carbonate. Earlier studies also achieved the successful solubilization of sub-Saharan low-grade African PRs (Nakamura et al. 2015).

When low-grade PRs are used as P resources, the heavy metal content must be considered. West low-grade African PRs from Togo, Senegal, and other countries have a high heavy metal content, such as Cd (Roberts 2014). As rice consumption in sub-Saharan Africa increased dramatically over the past 30 years, various initiatives related to sustainable rice production are underway (Johnson et al. 2019). The standard that the Codex Alimentarius Commission established for Cd content in polished rice is 0.4 mg kg^{-1}. Therefore, care must be taken to ensure that increased rice production using phosphate fertilizers is achieved with minimal transfer of heavy metals into rice. In conjunction with calcination, heat treatment can effectively remove heavy metals, such as Pb, Cd, and Cr, by chlorination and/or reduction volatilization when chloride or carbon are present (Matsuno et al. 2004). These technologies have been shown to be applicable to PRs (Kouzbour et al. 2019, Cichy et al. 2014) and should be implemented for low-grade PRs in sub-Saharan Africa.

Partial acidulation and high-temperature calcination can promote phosphate solubility of low-P-soluble PRs, but suitable processing methods differ based on their properties. Although substantial PR lists exist (e.g., Van Straaten 2002), they primarily focus on geological information, such as rock type, formulation age, and abundance. However, almost no studies exist in which the data were organized specifically to select a PR solubilization method. An inventory of the properties of local PRs, such as solubility and chemical composition, including heavy metals, will help select appropriate processing methods based on the characteristics of the low-grade PRs. Therefore, our study aimed to determine the mineralogical characteristics and solubilities of low-grade African PRs for agricultural use in different countries and to clarify the relationship between mineral properties and phosphate solubility. Additionally, the heavy metal content of low-grade PRs was evaluated from the perspectives of food safety and human health.

Materials and methods

1. Local African phosphate rocks

Ten local African PRs were collected from Minjingu (Tanzania), Matam (Senegal), Tilemsi (Mali), Lam-Lam (Senegal), Kodjari (Burkina Faso), Tahoua (Niger), Hahotoe (Togo), Sinda (Zambia), Evate (Mozambique), and Dorowa (Zimbabwe) with the assistance of on-site researchers (see Table 1). The first seven PRs (from Minjingu to Hahotoe) were sedimentary, whereas the PRs from Sinda and Dorowa were of igneous origin. Although the Evate PR origin was metamorphic (Davidson 1986), it was considered igneous for convenience due to high-temperature alteration.

2. Chemical and mineralogical analysis

The amount of available P depends on the type and amount of P-bearing minerals. The peak intensity, shift, and width of an X-ray diffraction peak in the same mineral provide information on the relative amount, elemental substitution, and crystallinity, respectively (Abouzeid 2008). The mineralogical composition was also reflected in the chemical composition.

The chemical compositions of the PRs were determined using the fundamental parameter method with X-ray fluorescence (XRF-FP, Rigaku, Model RIX3100). The mineral composition was determined by powder X-ray diffractometry (XRD, Bruker D8 Advance) at a current, voltage, 2θ step size, scan speed, and 2θ measurement range of 350 mA, 35 kV, 0.02°, 0.13 s per step, and 10°-65°, respectively.

Fluorapatite, a major constituent of African PRs, generates diffraction peaks corresponding to the (211), (112), (300), and (202) planes in the 2θ range of 31°-35° on the low-angle side. The (211) plane (2θ = 32°), which exhibits the highest intensity, was selected to automatically calculate crystallinities, such as the full width at half maximum (FHWM), crystallite size, and unit cell parameters a and c using the provided lattice-parameter-refinement function. Calculations were performed using francolite and fluorapatite for the PRs of sedimentary and igneous origins, respectively. The diffraction lines corresponding to the (211) and (112) planes were close to each other and were calculated after manual background correction.

The crystallite size (D) was calculated using the Scherrer equation.

$$D = \mathrm{K}\lambda/\beta\cos\theta_B, \quad (1)$$

where K and λ are the Scherrer constant (0.89) and wavelength of CuKα radiation of 1.5406 Å, respectively. β (rad) and θ_B are the full-width half maximum of the (211) plane and the angle corresponding to the (211) plane.

3. Thermal analysis

Thermogravimetry/differential thermal analysis (TG-DTA) provided relevant information about mineralogy (Abouzeid 2008). As weight loss, heat release (exothermic), and heat absorption (endothermic) can be measured simultaneously during heating using TG-DTA method, we can obtain information about the dehydration of crystal water, such as clay minerals, crandallite, wavellite, and carbonate decomposition with CO_2 release. To eliminate the influence of adhered water, the samples were dried at 100°C for one day or night before analysis. The TG-DTA was performed using a BRUKER TG-DTA2000SA instrument under N_2 flow (300 mL/min) by increasing the temperature from ambient conditions to 1,000°C at a rate of 20°C/min.

4. Phosphate solubility and heavy metal contents

This paper clarifies the relationship between phosphate solubility and chemical and mineralogical composition of PR. Because the solubility is affected by

Table 1. Deposit type and formation age of the phosphate rocks (PRs)

Country	Deposit name	Deposit type	Formulation age	Numerical age (Ma)	References
Tanzania	Minjingu	Sedimentary	Upper Pliocece or Pleistocene	3.6-0.01	Schlüter (1997), Van Straaten (2002)
Senegal	Matam	Sedimentary	Late Paleocene (Thanetian) to Early Eocene (Ypresian)	59.2-47.8	Prian (2014)
Senegal	LamLam	Sedimentary	early Middle Eocene	47.8-41.2	Prian (2014)
Mali	Tilemsi	Sedimentary	Eocece (Lutetian)	47.8-41.2	Pascal and Traore (1989), Hanon (1990)
Burkina Faso	Kodjari	Sedimentary	Neoproterozoic (660±8 million years)	660±8	Trompette (1989)
Niger	Tahoua	Sedimentary	Cretaceous to Eocene	145-33.9	Dumas (1971)
Togo	Hahotoe	Sedimentary	Late Ypresian - Early Lutetian	51.9-44.5	Johnson et al. (2010), Van Kauwenbergh & McClellan (1990)
Zambia	Sinda	Igneous	unknown	unknown	Sliwa (1991)
Mozambique	Evete	Metamorphic	970±23 million years	970±23	Davidson (1986)
Zimbabwe	Dorowa	Igneous	the late Paleozoic to Mesozoic eras	252-66	Fernandes (1989)

soil acidity, it was evaluated using various extractants such as water, citric acid, formic acid, and neutral ammonium citrate solution (FAO 2003). To measure the phosphate solubilities of the PRs, the study used the following extractants: water (W-P_2O_5), Petermann citrate solution (S-P_2O_5), 2% citric acid (C-P_2O_5), and neutral ammonium citrate (NCA-P_2O_5).

The total phosphate (T-P_2O_5) content of the PRs was determined by heating on a hotplate with a mixture of hydrochloric and nitric acids. After extraction, the phosphate content of each extract was measured using the vanadomolybdic acid method with a spectrophotometer (UV-1800, Shimadzu Corporation).

The heavy metal content of the PRs (i.e., the total As, Cd, Hg, Ni, Cr, and Pb) were determined as toxic components by inductively coupled plasma atomic emission spectroscopy (ICP-AES). Phosphate and heavy metal content were measured by fertilizer analysis method (National Institute for Agro-Environmental Sciences 1992).

Results

1. Chemical and mineralogical compositions of African PRs

Table 2 lists the chemical composition of the PRs, and Figure 1 shows their XRD patterns. The total P_2O_5 content of the PRs varied widely, ranging from 20.7% (Sinda) to 38.4% (Evate), as shown in Table 2. The F content ranged from 0.0% (Matam) to 3.45% (Evate). The loss on ignition (LOI) of the Matam PR (35.2%) was significantly higher than that of the other PRs because its major minerals, calcium hydrogen phosphate hydrate ($Ca(H_2PO_4)2•H_2O$) and brushite ($CaPO_3(OH)•2H_2O$), contain abundant crystal water. The SiO_2 content correlated negatively with the amount of P_2O_5. The SiO_2 content of the Kodjari- and Sinda-derived PRs exceeded 20% because of the presence of quartz, and augite and pargasite, respectively. The Al_2O_3 content was high in the Kodjari and Lam-Lam PRs due to the presence of wavellite and clinochlore, and crandallite and kaolinite, respectively. The Tilemsi, Tahoua, and Sinda PRs had high Fe_2O_3 contents due to goethite in the Tilemsi and Tahoua PRs, and koninckite in the Sinda PR. The MgO content was high in the Minjingu and Sinda PRs due to dolomite in the former and augite and pargasite in the latter.

Figure 1 shows XRD patterns acquired in a 2θ range of 31°-35°, and Table 3 lists the calculated (211)-plane FWHM, unit cell parameters *a* and *c*, and the crystallite size of the PRs, except for the Matam PR, which contains neither fluorapatite and francolite. All four diffraction peaks appearing in Figure 1 indicate the presence of fluorapatite or francolite and correspond to the (211), (112), (300), and (202) planes on the low-angle side. The (211) plane had the strongest peak.

Considering the PRs of sedimentary origin (Fig. 1), the (211) and (112) planes in the Minjingu and Tilemsi PRs were not clearly separated because of their relatively younger formation ages than other PRs. Notably, the (211) and (112) planes of the Minjingu PR were congruent. This was due to the higher CO_3^{2-} displacement rate of Minjingu PR, indicating that its crystal structure was similar to that of francolite. Carbonate-fluorapatite (francolite) is the principal mineral in phosphorites and sedimentary PRs. The CO_3^{2-} group is considered a part of the fluorapatite structure, substituting for the PO_4^{2-}groups in naturally occurring minerals (McConnell 1952, Altschuler et al. 1952, LeGeros et al. 1970).

The diffraction peak positions shifted higher for

Table 2. Chemical composition of the raw PRs

	Ig. loss	F	CaO	P_2O_5	SiO_2	Al_2O_3	Fe_2O_3	MgO	Na_2O	K_2O
	% (w/w)									
Minjingu	10.50	2.40	40.10	24.67	11.69	2.18	1.48	2.89	0.88	1.17
Matam	35.20	0.00	21.04	35.82	3.56	1.40	1.16	0.24	0.75	0.39
Tilemsi	5.85	2.19	38.83	27.81	10.78	3.02	6.88	0.35	0.38	0.30
Lam-Lam	7.40	2.58	36.91	29.85	9.38	7.64	4.29	0.14	0.12	0.10
Kodjari	5.26	2.02	32.58	24.52	23.85	6.40	3.55	0.48	0.11	0.48
Tahoua	4.75	2.57	39.49	28.73	9.01	2.66	10.53	0.24	0.17	0.13
Hahotoe	3.85	3.36	52.25	33.29	3.03	1.79	1.29	0.13	0.22	0.04
Sinda	2.10	0.65	35.75	20.70	20.94	3.01	7.95	5.68	0.49	0.43
Evate	0.20	3.45	56.47	38.40	0.46	0.16	0.10	0.02	0.02	0.02
Dorowa	0.70	1.87	55.88	36.51	1.88	0.23	1.54	0.42	0.31	0.03

sedimentary PRs with younger formation ages, except for those from Matam, which consisted of mainly hydroxyapatite (Fig. 1). This indicates that the crystal lattice spacing (d-spacing) decreased. The CO_3^{2-} substitution rate was higher in apatite with a younger formation age. The separation of the (211) and (112) peaks indicates that CO_3^{2-} is gradually removed from francolite as it transforms into fluorapatite. According to McClellan & Van Kauwenbergh (1991), younger PRs tend to have a higher proportion of CO_3^{2-} substituting for PO_4^{3-} and exhibit a tendency for a smaller lattice constant *a*. Based on this, Minjingu and Tilemsi were considered to be relatively young compared to other sedimentary PRs.

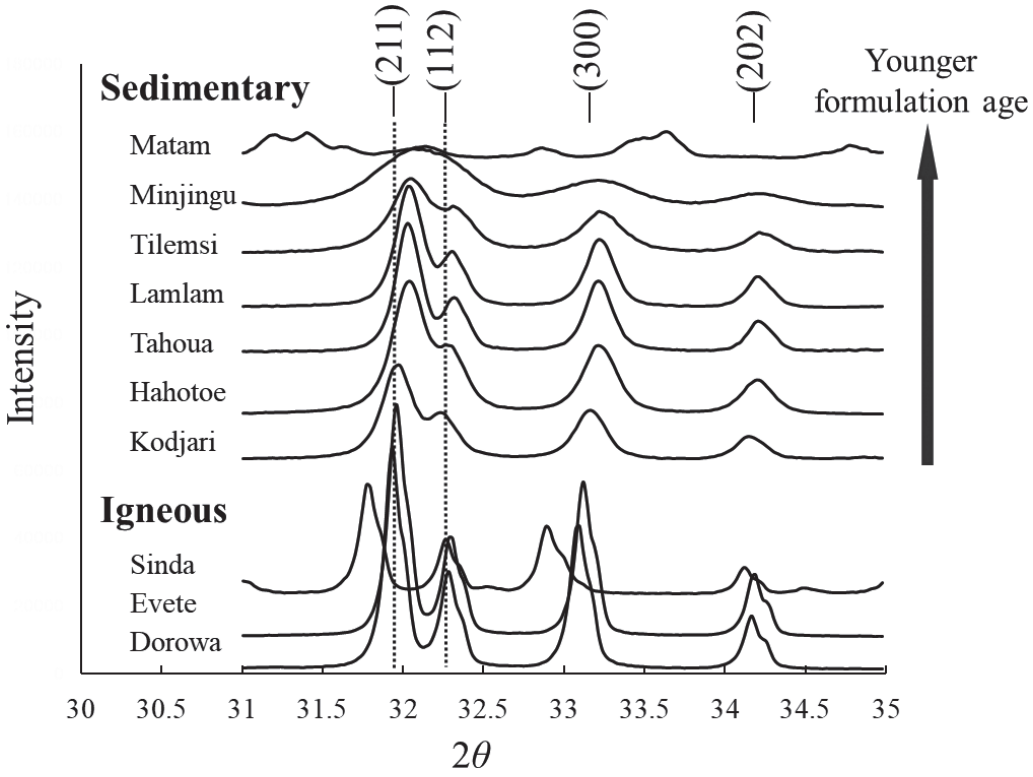

Fig. 1. X-ray diffractometry (XRD) patterns of phosphate rocks (PRs) in the 2θ range 31°-35°

Table 3. Full width at half maximum (FWHM), unit cell parameters (*a* and *c*), and crystallite size of the African PRs

	FWHM	*a*	*c*	Crystallite size
	(°)	(10^{-1} nm)		
Minjingu	0.653	9.3453	6.8964	151.2
Tilemsi	0.360	9.3472	6.8804	282.2
Lam-Lam	0.163	9.3439	6.8843	516.3
Kodjari	0.198	9.3511	6.8864	445.4
Tahoua	0.151	9.3466	6.8813	521.9
Hahotoe	0.223	9.3433	6.8881	406.9
Sinda	0.104	9.4448	6.8724	645.5
Evate	0.101	9.3784	6.8827	824.5
Dorowa	0.098	9.3927	6.8876	792.4

2. Thermal analysis of African PRs

Figures 2-4 show the thermogravimetric curves of the PRs acquired by TG-DTA. The weight loss characteristics of each PR are described below.

The Minjingu PR was characterized by a significant weight loss (10.5%; XRF-FP data in Table 2) and high concentrations of MgO (2.9%) and K_2O (1.2%). Although the phosphate in this PR was francolite, the weight loss at 1,000°C was relatively large (9.3%; Fig. 2). The weight loss was particularly large in the 600°C-800°C ranges; these were attributed to dehydration of muscovite and decarbonation of dolomite ($CaMg(CO_3)_2$) (Guggenheim et al. 1987, Ozao et al. 1986).

The TG-DTA profile of the Matam PR (Fig. 3) differed considerably from those of the other PRs, as evidenced by its distinct endothermic weight losses at 170, 330, and 830°C. The weight loss at 170°C was ascribed to the dehydration of dihydrate gypsum ($CaSO_4 \cdot 2H_2O$), whereas that at 330 and 830°C was attributed to the dehydration of hydroxyapatite (Bouzit et al. 2019, Matsuno 1985).

The weight loss of the Tilemsi PR (5.9% at 1,000°C) increased monotonically to 1,000°C and was similar to that of the Kodjari PR (Fig. 2). This was attributed to the dehydration of crystalline water in muscovite ($KAl_2(AlSi_3O_{10})(OH)_2$), $Ca(Mg_2Al)(Al_{2.8}Si_{1.2})O_{10}(OH)_2$, kaolinite ($Al_2(Si_2O_5)(OH)_4$), and goethite ($Fe_2O_3 \cdot H_2O$). Particularly, the weight loss with endothermy at ~300°C was ascribed to the dehydration of goethite (Guggenheim et al. 1987, Wang et al. 2011, Pozas et al. 2004).

The Lam-Lam PR exhibited a weight loss of 4.8% at 1,000°C, with the largest drop occurring between 400 and 600°C. This is attributed to the dehydration of crystalline water in crandallite ($CaAl_3(OH)_6(PO_3(O_{0.5}(OH)_{0.5}))_2$) and kaolinite (Frost et al. 2012, Wang et al. 2011).

The Kodjari PR lost weight monotonically to 1,000°C, with a weight loss of 4.7% at 1,000°C. This weight loss is ascribed to the dehydration of crystalline water in chlorite ($(Mg_5Al)(Si,Al)_4O_{10}(OH)_8$) and wavellite ($Al_3(PO_4)_2(OH)_3(H_2O)_5$) (Shirozu 1980, Nokolova et al. 2018).

The Tahoua PR exhibited a weight loss rate of 4.0% at 1,000°C. The chemical and mineral composition analyses indicated that the Tahoua PR comprised the highest Fe_2O_3 concentration (10.5%) among the PRs due to its higher goethite (FeO(OH)) content than that of the other PRs. Furthermore, weight loss with endothermy at approximately 300°C, identical to that of the Tilemsi PR, was observed due to the dehydration of goethite (Bouzit et al. 2019).

The Hahotoe PR also lost weight monotonically up to 1,000°C, resulting in a value of 3.7% at 1,000°C. The TG-DTA pattern of the Sinda PR (Fig. 4; weight loss of 2.04% at 1,000°C) was similar to that of the Dorowa PR. The largest weight change was observed between 600 and 780°C. The Dorowa PR exhibited a weight loss of 0.8% at 1,000°C (Fig. 4). Characteristic weight loss was observed in the same temperature range as Sinda PR. These were likely due to the decarbonation of calcite

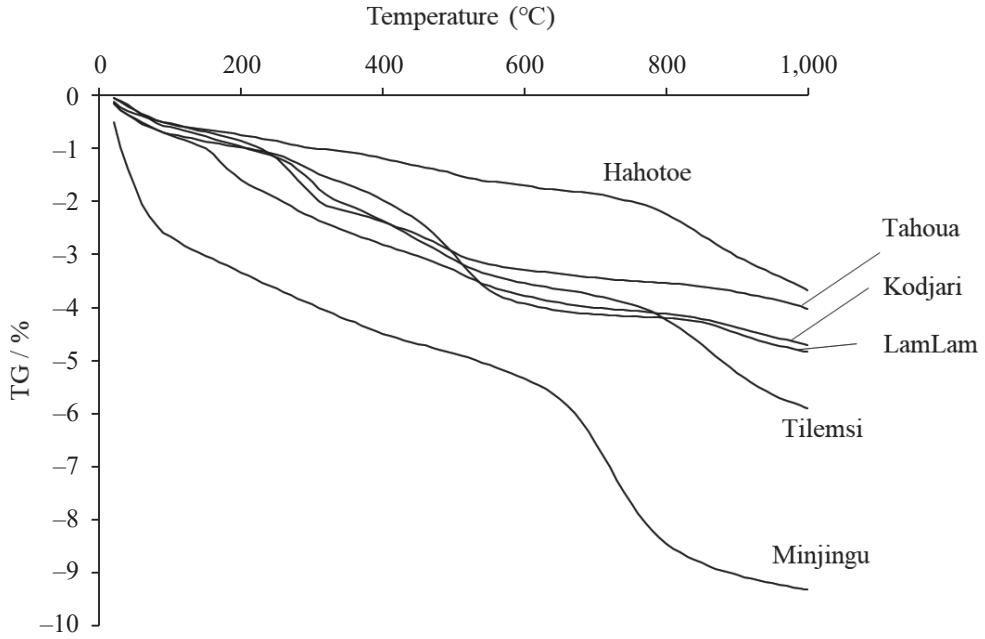

Fig. 2. Thermogravimetric curves of sedimentary-origin PRs excluding the Matam PR

($CaCO_3$), as identified by XRD (Yamaguchi et al. 2015).

As indicated by the XRD results, Evate PR comprised the highest concentration of fluorapatite ($Ca_5(PO_4)_3F$) among all PRs (see Fig. 1). Therefore, it exhibited a weight loss of only 0.27% at 1,000°C.

3. Heavy metal contents of the African PRs

Table 4 lists the heavy metal contents of the PRs. The Cd content was high in the Matam, Lam-Lam, and Hahotoe PRs. The Cr content of the Matam, Lam-Lam, and Hahotoe PRs was also relatively high, as was the Sr

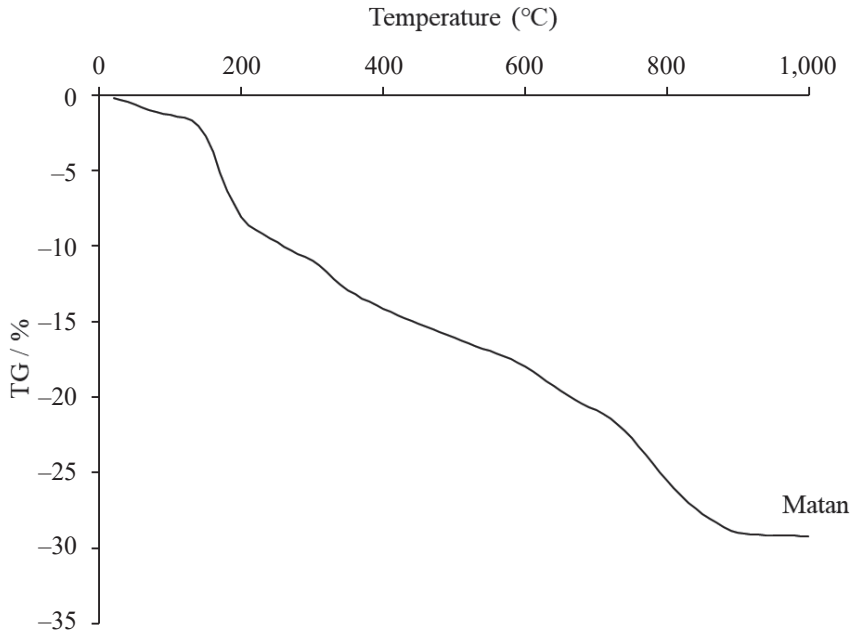

Fig. 3. Thermogravimetric profile of the Matam PR

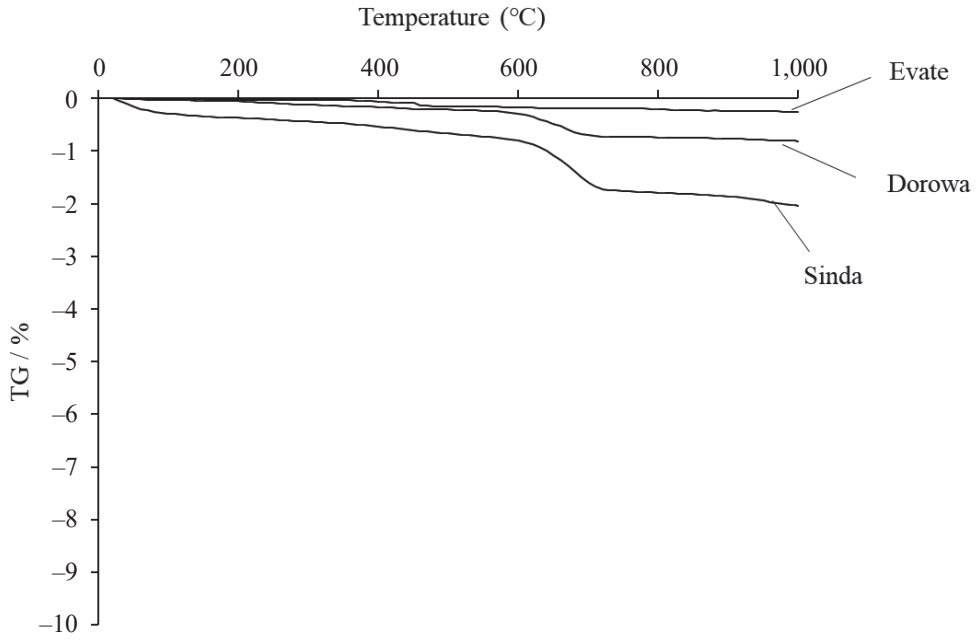

Fig. 4. Thermogravimetric curves of PRs of igneous origin

content in the Minjingu and Sinda PRs. Additionally, uranium (U) was detected in the PRs sourced from Minjingu, Tahoua, Hahotoe, Kodjari, and Evate.

4. Phosphate solubility of the African PRs

Table 5 shows the phosphate solubilities of the PRs in different solutions. The total phosphate content varied from 17.2% (Sinda) to 40.6% (Evate). These values are consistent with those of the XRF results. The W-P_2O_5 values were generally low, except for the Matam PR, which exhibited the highest value among the PRs due to hydroxyapatite being its major phosphate mineral (62% of its T-P_2O_5 value). Furthermore, the S-P_2O_5 and NCA-P_2O_5 values showed trends similar to those of W-P_2O_5, with the Matam PR exhibiting the highest values of S-P_2O_5 (79.9% of T-P_2O_5) and NCA-P_2O_5 (77.3% of T-P_2O_5) among the PRs, the other PRs had extremely low phosphate solubilities (S-P_2O_5, 0.1% to 3.5% of T-P_2O_5; NCA-P_2O_5, 0.1% to 2.9% of T-P_2O_5). However, the C-P_2O_5 data differed from those derived from the other extracts, with relatively high amounts of phosphate extracted from all the PRs. Particularly, the C-P_2O_5 content was higher in the Tilemsi (13.8%), Minjingu (17.6%), and Matam PRs (27.7%) than in the others.

Table 4. Heavy metal contents of the African PRs

	As	Cd	Hg	Ni	Cr	Pb	SrO**	U_3O_8**
	(mg kg^{-1})							
Minjingu	9	< 0.5	< 0.1	< 5	11	1	8050	490
Matam	2	110	< 0.1	33	130	3	810	-
Tilemsi	8	0.9	< 0.1	15	9	6	1120	-
Lam-Lam	4	37	< 0.1	67	350	< 1	4460	-
Kodjari	7	< 0.5	< 0.1	< 5	13	2	1490	10
Tahoua	9	0.6	< 0.1	5	6	2	1480	50
Hahotoe	12	22	< 0.1	10	53	3	550	110
Sinda	16	< 0.5	< 0.1	< 5	7	3	5200	-
Evate	25	< 0.5	< 0.1	< 5	< 5	4	3020	50
Dorowa	2	< 0.5	< 0.1	< 5	< 5	2	3750	-

* ' < ' indicates that the value was below the lower limit of quantification.
**quantitated by XRF-FP method

Table 5. Phosphate solubilities of the African PRs

	T-P_2O_5	W-P_2O_5	S-P_2O_5	C-P_2O_5	NCA-P_2O_5
	(weight %)				
Minjingu	25.2	< 0.01	0.32	17.6	0.72
Matam	38.9	24.10	31.10	27.7	30.08
Tilemsi	26.2	< 0.01	0.52	13.8	0.19
Lam-Lam	27.9	< 0.01	0.62	10.2	0.14
Kodjari	25.1	0.02	0.87	9.1	0.10
Tahoua	26.6	0.02	0.41	9.2	0.12
Hahotoe	35.4	0.02	0.39	10.6	0.13
Sinda	17.2	< 0.01	0.09	6.3	0.11
Evate	40.6	0.02	0.30	6.8	0.14
Dorowa	38.4	< 0.01	0.04	4.9	0.02

* ' < ' indicates that the value was below the lower limit of quantification.
** T-P_2O_5: Total phosphate in PRs; W-P_2O_5, S-P_2O_5, C-P_2O_5, and NCA-P_2O_5: phosphates soluble in water, Petermann citrate solution, citric acid, and neutral ammonium citrate, respectively.

Discussion

1. Mineralogical properties of the African PRs

Based on the mineral composition results obtained through the TG-DTA and XRD analyses, the ten African PRs analyzed here were broadly classified into the five groups shown in Table 6.

Group 1: Primarily comprising hydroxyapatite (Matam);
Group 2: Containing impurities related to quartz and clay minerals (Kodjari and Lam-Lam);
Group 3: Containing impurities, such as iron hydroxide, quartz, and clay minerals (Tahoua and Tilemsi);
Group 4: Containing carbonate-type impurities, such as calcite and dolomite (Minjingu, Dorowa, and Sinda);
Group 5: Containing few impurities (Hahotoe and Evate).

Figure 5 shows the relationship between the peak position of the (211) plane and the unit cell parameter *a* of francolite and fluorapatite. Regardless of the origin, sedimentary or igneous, the peak position correlated negatively with *a*. The values of *a* for the sedimentary PRs were close to that of francolite (9.346 Å), and the variation was small even when 2θ was between 32.00° and 32.07°. According to the XRD analysis (Table 3), the value of *a* for the Kodjari PR (9.3511) was higher than

Table 6. Identified minerals in the raw PRs

	Group	Phosphate-containing minerals	Other minerals
Minjingu	4	francolite	dolomite, micas, quartz, orthoclase
Matam	1	hydroxyapatite, brushite, $Ca(Al,Fe)H(PO)\cdot 4H_2O$	anhydrite, gypsum, quartz
Tilemsi	3	fluorapatite	quartz, goethite, micas, kaolinite
Lam-Lam	2	fluorapatite, crandallite	quartz, kaolinite
Kodjari	2	fluorapatite, wavellite	quartz, micas, clinochlore
Tahoua	3	fluorapatite	quartz, goethite
Hahotoe	5	fluorapatite	quartz
Sinda	4	fluorapatite, koninckite	augite, calcite, potassicpargasite
Evate	5	fluorapatite	
Dorowa	4	fluorapatite, koninckite, $Ca_{10}(PO_4)_5\cdot CO_3(OH)F$	calcite

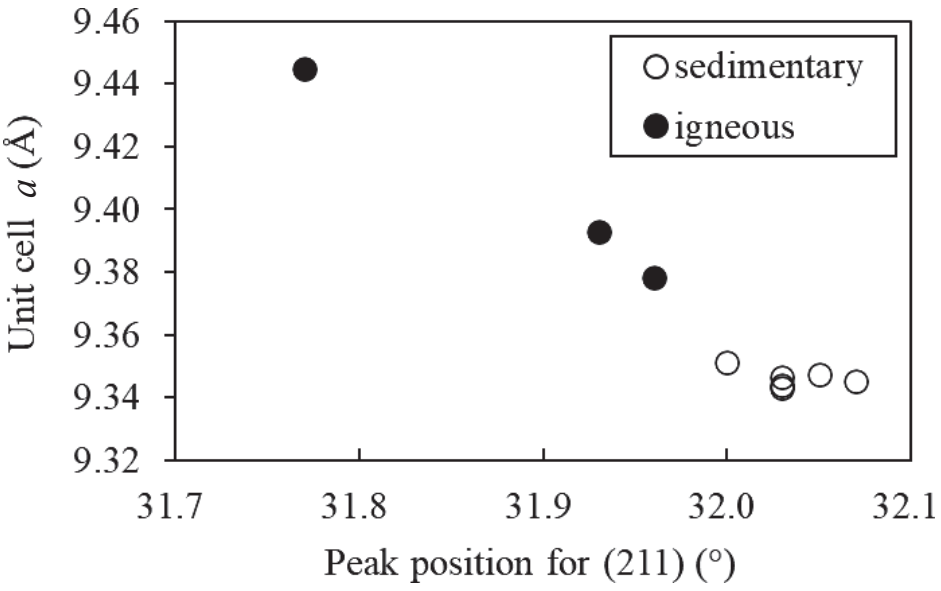

Fig. 5. Relationship between XRD peak position corresponding to the (211) plane and unit cell parameter *a*

those for the other sedimentary PRs, possibly because of the lower CO_3^{2-} substitution rate at the phosphate ion sites.

Of the igneous PRs, the Sinda PR exhibited a greater shift in its XRD pattern to the low-angle side than the Evate and Dorowa PRs, with *a* value of 9.4448, the highest among the analyzed PRs. In addition, this PR exhibited the broad peak. As the igneous PRs were subjected to high temperatures, they became CO_3^{2-}-free or had a low rate of CO_3^{2-} substitution in their crystal structures. The SrO concentrations in the Sinda, Evate, and Dorowa PRs were 5,200, 3,020, and 3,750 mg kg^{-1}, respectively, suggesting a significant shift in the XRD pattern of the Sinda PR to the low-angle side due to the replacement of Ca sites with Sr, which has a large ionic radius.

Figure 6 shows the dependence of cell parameter *a* on the angular difference of the XRD diffraction peaks ($\Delta 2\theta$) between the (004) and (410) planes of francolite and fluorapatite. A positive correlation was obtained between $\Delta 2\theta$ and cell parameter *a*. However, the variation in the $\Delta 2\theta$–*a* data for the francolites of sedimentary origin here was small. Matthews & Nathan (1977) showed that the $\Delta 2\theta$ values of francolite correlate negatively with the CO_3^{2-} ion content. Furthermore, McClellan & Van Kauwenberch (1991) reported a negative correlation between carbonate ions (CO_3^{2-}) and cell parameter *a* for francolite. Therefore, the difference in the CO_3^{2-} ion content is expected to be small for the francolites of sedimentary origin investigated in this study.

2. Influence of mineral properties of PRs on solubility

The neutral ammonium citrate (NCA), 2% CA, and water extraction methods were used to evaluate phosphate solubility when the PRs were directly applied. Although NCA-soluble P was directly proportional to CA-soluble P, the high CA-soluble P content of the sedimentary PRs, except for the Minjingu PR, did not necessarily indicate a high NCA-soluble P content, suggesting that the factors affecting the rate of NCA solubility differed from those affecting the rate of CA solubility.

The phosphate solubility in the PRs was evaluated using different solvents; however, the amount of dissolved phosphate was low for most PRs except for CA. Studies determined that the CA-soluble fraction is the soluble P fraction most associated with phosphate fertilizer efficacy (Braithwaite et al. 1989), indicating the viability of the direct application of PRs. However, in terms of phosphate fertilizer production, the higher the CA-soluble phosphate, the higher the amount of phosphate dissolved using the acid dissolution and calcination methods. Therefore, the amount of CA-dissolved phosphate indicates the feasibility of direct application and the effectiveness of fertilizer production.

Figure 7 shows the relationship between the crystallite size and the ratio of citrate-soluble phosphate (C-P_2O_5) to total phosphate (T-P_2O_5) in francolite and fluorapatite, as determined using Scherrer's equation. Regardless of the PR origin, the larger the crystallite size was, the lower the phosphate solubility. Although some

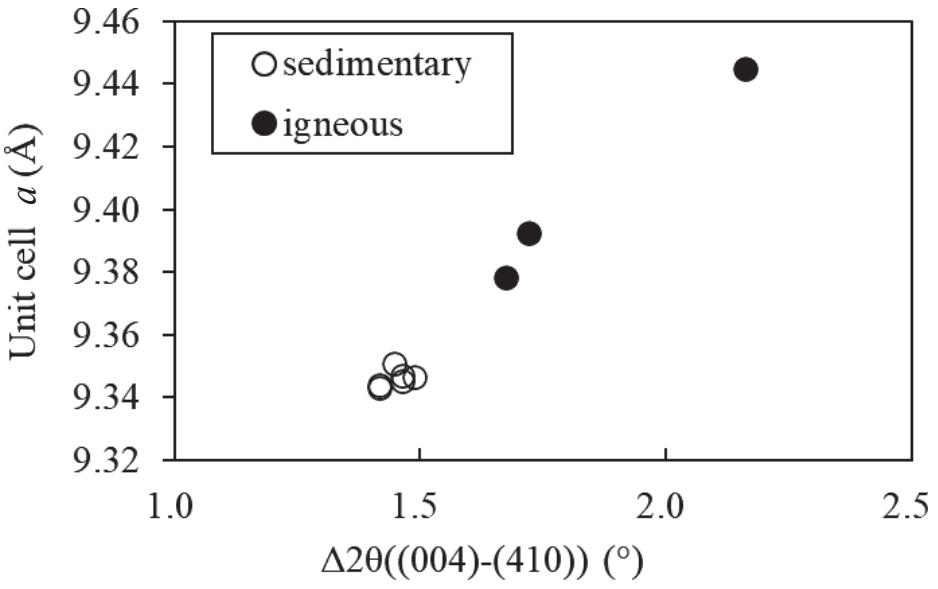

Fig. 6. Relationship between a and $\Delta 2\theta$ based on the peaks representing the (004) and (410) planes

variations were observed, the overall correlation between these parameters was negative. We assume the phosphate solubility of African PRs ($C\text{-}P_2O_5/T\text{-}P_2O_5$) was controlled by the crystallite size of the PRs.

Phosphate solubility varies among the PRs for several reasons. PRs contain apatites, such as francolite and fluorapatite, and other phosphate minerals, such as wavellite (Kodjari PR) and crandallite (Lam-Lam PR). Carbonates such as dolomite (Minjingu PR) and calcite (Sinda and Dorowa PRs) inhibit phosphate dissolution in acidic solutions such as CA.

3. Selecting an appropriate fertilization process based on the mineral and chemical properties of PRs

Among the PRs investigated here, the Matam PR comprised the highest total phosphate content (38.9%) and had an extremely high percentage of soluble phosphate ($W\text{-}P_2O_5$ and $C\text{-}P_2O_5$: 62% and 71.2% of $T\text{-}P_2O_5$, respectively). Generally, the standard for PRs used in the production of phosphate fertilizers is a phosphate content of at least 37% P_2O_5 (equivalent to 80 bone phosphate of lime (BPL); 1% P_2O_5 = 2.185% BPL) (Van Kauwenbergh 2010). Therefore, the Matam, Evete, and Dorowa PRs were not classified as low-grade. Direct application effectiveness of PRs with 30% of $C\text{-}P_2O_5$ was confirmed in earlier studies (FAO 2004). Matam PR (Group 1) is also sufficiently effective for direct applications. The Minjingu and Tilemsi PRs also exhibit high $C\text{-}P_2O_5$ values.

Compared to $T\text{-}P_2O_5$ for PRs other than for Matam, Minjingu, and Tilemsi, the $C\text{-}P_2O_5$ rate was 12.8%-36.6% ($C\text{-}P_2O_5/T\text{-}P_2O_5$). For effective utilization, low-grade PRs must be converted into phosphate fertilizers. Partial acidulation is effective for converting low-grade PRs into acid-soluble phosphate fertilizers and was tested using PRs from various regions (Zapata 2003, Cicek et al. 2020, Saied et al. 2022). Partial acidulation is a simple method that can be used for low-grade PR. However, the amount of soluble phosphate depends on the chemical composition of PRs (e.g., Van Kauwenbergh 1995). In particular, PRs with high Fe and Al contents have low soluble phosphate content (Hammond et al. 1989). Therefore, partial acidulation may be an effective method for Minjingu (Group 4), Hahotoe (Group 5), Evete (Group 4), and Dorowa (Group 4) PRs, which have low Fe and Al contents.

Calcination technology was developed to solubilize phosphate in low-grade PRs by heating and adding carbonate materials (Akiyama 1988, Nakamura et al. 2015). In addition to solubilizing phosphate in PRs, the heavy metal content of phosphate fertilizers can be reduced by vaporizing heavy metals, particularly Cd, via high-temperature calcination (Abbes et al. 2020). Among the PRs used here, Matam, Lam-Lam, and Hahotoe PRs had the highest heavy metal content (Cd, Ni, and Cr). Calcination is effective in converting PRs into phosphate fertilizers and found to be effective for Kodjari PR with high Fe and Al contents (Nakamura et al. 2015). Therefore, calcination may be feasible for Tilemsi (Group 3), Lam-Lam (Group 2), Kodjari (Group 2), Tahoua (Group 3), and Sinda (Group 4) PRs, which are unsuited to acid solubilization.

Therefore, an optimal method for converting

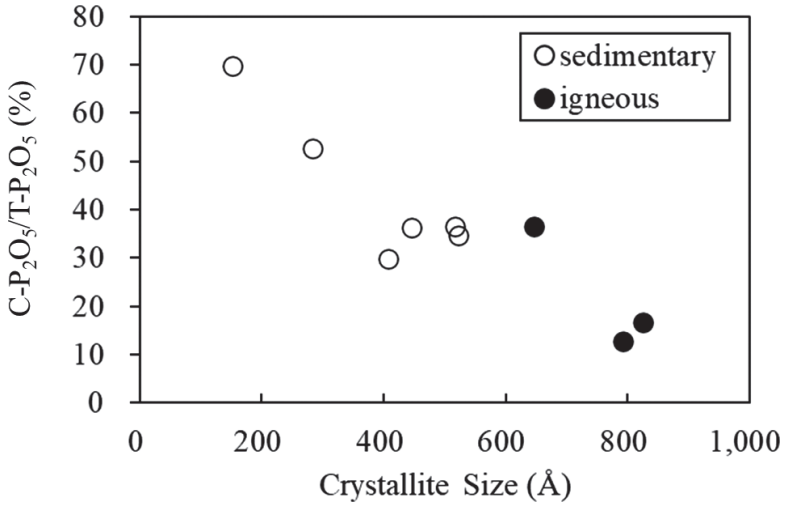

Fig. 7. Relationship between crystal size and $C\text{-}P_2O_5/T\text{-}P_2O_5$ rate
$T\text{-}P_2O_5$: total phosphate in PRs; $C\text{-}P_2O_5$: citric acid-soluble phosphate

low-grade PRs into phosphate fertilizers can be selected based on their mineral, chemical, soluble phosphate, and heavy metal contents. The information collected here will enhance the utilization of PRs via direct application and fertilizer production through the above technologies.

Conclusion

Detailed chemical and mineralogical analysis can be used to develop guidelines for suitable processing to produce cheaper P fertilizers.

As phosphate solubility improvement and suitable processing for each PR differed, the phosphate solubilities of ten low-grade African PRs with different properties were correlated with their chemical and mineralogical compositions.

We obtained the following results.

(1) The phosphate solubility of low-grade African PRs (i.e., C-P_2O_5/T-P_2O_5) is controlled by the crystallite sizes of francolite and fluorapatite, regardless of the origin of the PR (sedimentary or igneous). Based on the mineral composition, the ten analyzed low-grade African PRs were classified into five groups, and appropriate processing for solubilization determined for each group.

(2) Low-grade PRs (Group 1), which mainly consist of hydroxyapatite, can be applied directly to agricultural land with careful consideration of their heavy metal content.

(3) Low-grade PRs (Groups 4 and 5) with low Fe and Al contents are suitable for partial acidulation because they undergo minimal P-fixation reactions during the acid decomposition process.

(4) Low-grade PRs (Groups 2, 3, and 4) with high Fe, Al, and heavy metal contents are believed to require solubilization through high-temperature calcination using fluxing additives, such as K and Na carbonates. The resulting alkaline minerals have high phosphate solubilities. Further, heavy metals, particularly Cd, can be removed via vaporization.

Acknowledgements

This study was supported by a SATREPS grant (Project on the establishment of the model for fertilizing cultivation promotion using Burkina Faso PR) funded by the Japan International Cooperation Agency (JICA) and the Japan Science and Technology agency (JST).

References

Abbes, N. et al. (2020) Thermal beneficiation of Sra Ouertane (Tunisia) low-grade phosphate rock. *Minerals*, **10**, 937.

Abd El-Halim, A. A. & Omae, H. (2019) Examination of nanoparticulate phosphate rock as both a liming agent and phosphorus source to enhance the growth of spinach in acid soil. *Soil Sci. Plant Nutr.*, **65**, 386-392. doi.org/10.1080/00380768.2019.1620082

Abouzeid, A. M. (2008) Physical and thermal treatment of phosphate ore-An overview. *Intl. J. Miner. Process.*, **85,** 59-84. doi.org/10.1016/j.minpro.2007.09.001

Adediran, J. A. & Sobulo, R. A. (1998) Agronomic evaluation of phosphorus fertilizers developed from Sokoto rock phosphate in Nigeria. *Commun. Soil Sci. Plant Anal.*, **29**, 2415-2428.

Akiyama, T. (1988) Calcination reaction of Brazilian aluminum phosphate ore with calcium carbonate. Nihon Dojou Hiryougaku Zasshi (*Jpn. J. Soil Sci. Plant Nutr.*), **59**, 260-265 [In Japanese with English summary].

Altschuler, Z. S. et al. (1952) X-ray evidence of the nature of the carbonate-apatites. *Bull. Geol. Soc. Am*., **63**,1230-1231.

Appleton, J. D. (2002) Local phosphate resources for sustainable development in sub-Saharan Africa. *In* British Geological Survey Report, CR/02/121/N., p. 134.

Bixby, D. W. (1980) Sulfur requirements of the phosphate fertilizer industry. *In* Khasawneh, F. E. et al. (eds.), The role of phosphorus in agriculture. American Society of Agronomy, Crop Science Society of America, and Soil Science Society of America, Wisconsin, USA, pp. 129-150.

Bouzit, S. et al. (2019) Characterization of natural gypsum materials and their composites for building applications. *Appl. Sci.*, **9**, 2443.

Braithwaite, A. C. et al. (1989) Some factors associated with the use of the extractants 2% citric acid and 2% formic acid as estimators of available phosphorus in fertiliser products. *Fert. Res.*, **19**, 175-181.

Chien, S. H. & Menon, R. G. (1995) Factors affecting the agronomic effectiveness of phosphate rock for direct application. *Fert. Res.*, **41**, 227-234.

Chtouki, M. et al. (2022) A phospho-compost biological-based approach increases phosphate rock agronomic efficiency in faba bean as compared to chemical and physical treatments. *Environ. Sci. Pollut. Res*., **29**, 74012-74023. https://doi.org/10.1007/s11356-022-21087-z

Cicek, H. et al. (2020) Partial acidulation of rock phosphate for increased productivity in organic and smallholder farming. *Sustainability*, **12**, 607.

Cichy, B. et al. (2014) Cadmium in phosphate fertilizers; ecological and economical aspects. *CHEMIK*, **68**, 837-842.

Davidson, D. F. (1986) Phosphate resources of Mozambique based on available data. Final Report to UN/DTCD, INT/80-R45. United Nations, New York.

Dumas, M. C. (1971) Projet des phosphate de Tahoua- Niger, Rapport sur la phase I. Report of Watts, Griffis, and McOuat to the Canadian International Development Agency (CIDA), Toronto, Canada.

FAO (2004) Use of phosphate rocks for sustainable agriculture. FAO fertilizer and plant nutrition bulletin 13, FAO, Rome.

Fernandes, T. R. C. (1989) Dorowa and Shawa: late Palaeozoic to Mesozoic carbonatite complexes in Zimbabwe. *In* A. H. J. Notholt, R. P. Sheldon, and D. F. Davidson (eds), Phosphate deposits of the world. 2. Phosphate rock resources. 171-175. Cambridge University Press.

Frost, R. L. et al. (2012) Thermal stability of crandallite

CaAl3(PO4)2(PH)5•(H2O). *J. Therm. Anal. Calorimetry*, **107**, 905-909.

Fukuda, M. et al. (2013) Ineffectiveness of directly applied Burkina Faso phosphate rock on rice growth. *Soil Sci. Plant Nutr.*, **59**, 403-409.

Guggenheim, S. et al. (1987) Muscovite dihydroxylation: High-temperature studies. *Am. Mineral.*, **72**, 537-550.

Hammond, L. L. et al. (1986) Agronomic value of unacidulated and partially acidulated phosphate rocks indigenous to the tropics. *Adv. Agron.*, **40**, 89-140.

Hammond, L. L. et al. (1989) Solubility and agronomic effectiveness of partially acidulated phosphate rocks as influenced by their iron and aluminium oxide content. *Fert. Res.*, **19**, 93-98.

Hanon, M. (1990) Notice explicative sur la carte de geologique de L'Ader Doutchi, Ministere des Mines et de L'Energie, Direction des Recherches Geologiques et Minieres, Niamey Niger. 36 pp.

Johnson, J. M. et al. (2019) Near-infrared, mid-infrared or combined diffuse reflectance spectroscopy for assessing soil fertility in rice fields in sub-Saharan Africa. *Geoderma*, **354**, 113840.

Johnson, A. K. et al. (2010) Le basin sedimentable a phosphate du Togo (Maastrichtian-Eocene)- stratigraphie, environments et evolution. *J. Aft. Earth Sci.*, **30**, 183-200.

Kouzbour, S. et al. (2019) Comparative analysis of industrial processes for cadmium removal from phosphoric acid: A review. *Hydrometallurgy*, **188**, 222-247. doi.org/10.1016/j.hydromet.2019.06.014.

LeGeros, R. Z. et al. (1970) Spectral properties of carbonate in carbonate-containing apatites. *In* E. L. Grove & A. J. Perkins (eds.), Developments in Applied Spectroscopy, Vol. 7B, Plenum Press, New York. pp. 3-12.

Liu, R. & Lal, R. (2015) Potentials of engineered nanoparticles as fertilizers for increasing agronomic productions. A review. *Sci. Total Environ.*, **514**, 131-139. doi:10.1016/j.scitotenv.2015.01.104.

MacDonald, G. K. et al. (2011) Agronomic phosphorus imbalances across the world's croplands. *Proc. Natl. Acad. Sci.*, **108**, 3086-3091.

Matsuno, M. et al. (2004) Analysis of reaction and mechanism in heavy metal voltalization of incinerator fly ash roasting. *Shigen to Sozai*, **120**, 521-526 [In Japanese with English abstract].

Matsuno, S. (1985) Bound water in hydroxyapatite prepared by wet process. *Nippon Kagaku Kaisi*, **1985**, 858-865 [In Japanese].

Matthews, A. & Nathan, Y. (1977) The decarbonation of carbonate-fluorapatite (francolite). *Am. Mineral.*, **62**, 565-573.

McClellan, G. H. & Van Kauwenberch, S. J. (1991) Mineralogical and chemical variation of francolites with geological time. *J. Geol. Soc.*, **148**, 809-812.

McConnell, D. (1952) The problem of the carbonate apatites. IV. Structural substitutions involving CO_3 and OH. *Bull. Soc. Fr. Minér. Cristallogr.*, **75**, 428-445.

Mokwunye, A. et al. (1986) Phosphate reactions with topical African soils. *In* Mokwunye, A. U. & Vlek, P. L. G. (eds), Management of nitrogen and phosphorus fertilizers in sub-Saharan Africa, Martinus Nijhoff Publishers, Springer Dordrecht, Netherlands, pp. 253-281.

Nakamura, S. et al. (2013) Potential utilization of local phosphate rocks to enhance rice production in sub-Saharan Africa. *JARQ*, **47**, 353-363.

Nakamura, S. et al. (2015) Solubilization of Burkina Faso phosphate rock through calcination method. *Jpn. J. Soil Sci. Plant Nutr.*, **86**, 534-538 [In Japanese].

National Institute for Agro-Environmental Sciences (1992) *Fertilizer Analysis Methods.* Japan Fertilizer & Feed Inspection Association (JFFIA), Tokyo [In Japanese].

Nishigaki, T. et al. (2021) Soil phosphorus retention can predict responses of phosphorus uptake and yield of rice plants to P fertilizer application in flooded weathered soils in the central highlands of Madagascar. *Geoderma*, **402**, 115326.

Nokolova, R. et al. (2018) Fluorwavellite from Petro shnitsa river valley, Republic of Macedonia. *Bulg. Chem. Commun.*, **50**, Special Issue J, 208-214.

Ozao, R. et al. (1986) Some properties of Ca-rich dolomites. *Gypsum & Lime*, **201**, 79-88 [In Japanese with English abstract].

Pascal, M. & Traore, H. (1989) Eocene Tilemsi phosphorite deposits, eastern Mali. *In* Notholt AJG, Sheldon RP and DF (eds) Phosphate deposits of the world. Vol. 2 Phosphate rock resources, Cambridge University Press, Cambridge, UK, pp. 226-232.

Pozas, R. et al. (2004) Acicular iron nanoparticles protected against sintering with aluminium oxide. *Boletin La Sociedad Española de Cerámica Vidrio*, **43**, 796-800.

Prian, J. (2014) Phosphate Deposits of the Senegal-mauritania-guinea Basin (West Africa): A review. Procedia Engineering, **83**, 27-36.

Roberts, T. L. (2014) Cadmium and phosphorus fertilizers: The issues and the science. *Procedia Eng.*, **83**, 52-59.

Rodrigues, N. A. et al. (2024) New approaches for solubilization of phosphate rocks through solid-state fermentation by optimization of oxalic acid production. *Biores. Tech.*, **408**, 131165. doi.org/10.1016/j.biortech.2024.131165.

Sagnon, A. et al. (2022) Amendment with Burkina Faso phosphate rock-enriched composts alters soil chemical properties and microbial structure, and enhances sorghum agronomic performance. *Sci. Rep.*, **12**, 13945. https://doi.org/10.1038/s41598-022-18318-1

Saied, H. S. H. et al. (2022) Chemical evaluation of partially acidulated phosphate rocks and their impact on dry matter yield and phosphorus uptake of maize. *Saudi J. Biol. Sci.*, **29**, 3511-3518.

Saito, K. et al. (2019) Yield-limiting macronutrients for rice in sub-Saharan Africa. *Geoderma*, **338**, 546-554.

Schlüter, T. (1997) *Geology of East Africa.* Gebrueder Borntraeger, Berlin-Stuttgart.

Sedogo, P. M. et al. (1991) Utilization efficace des engrais azotés pour une augmentation de la production vivrière: L'expérience du Burkina Faso. *In* Mokwunye A. U. (ed), Alleviating soil fertility constraints to increased crop production in West Africa, Kluwer Academic Publishers, Netherlands, pp. 115-123 [In French with English abstract].

Shirozu, H. (1980) Variation of DTA and TG curves for Mg-chlorites. *Clay Sci.*, **5**, 237-244.

Sliwa, A. S. (1991) Phosphate resources of Zambia and progress in their exploration. *Fert. Res.*, **30**, 203-212. doi.org/10.1007/BF01048655

Trompette, R. (1989) Phosphorites of northern Volta Basin

(Burkina Faso, Niger, and Benin) *In* Notholt AJG, Sheldon RP and DF Davidson (eds.) Phosphate deposits of the world. Vol. 2. Phosphate rock resources, Cambridge University Press. Cambridge. UK, pp. 214-218.

Van Kauwenbergh, S. J. (1995) Mineralogy and characterization of phosphate rock. *In* Dahanayake, K. et al. (eds), Direct application of phosphate rock and appropriate technology fertilizer in Asia - what hinders acceptance and growth, Institute of Fundamental Studies, Kandy, Sri Lanka, pp. 29-47.

Van Kauwenbergh, S. J. (2010) *World Phosphate Rock Reserves and Resources*. IFDC, Alabama, USA.

Van Kauwenbergh, S. J. & McClellan, G. H. (1990) Comparative geology and mineralogy of the southeastern United States and Togo phosphorites, *In* Notholt, A. J. G., and Jarvis, I. (eds.), Phosphorite research and development: Geological Society of London Special Publication 52, pp. 139-155. doi. org/10.1144/gsl.sp.1990.052.01.10

Van Straaten, P. (2002) *Rocks for Crops*: *Agrominerals of sub-Saharan Africa, ICRAF, Nairobi, Kenya*, 338 pp.

Wang, H. et al. (2011) Characterization and thermal behavior of kaolin. *J. Therm. Anal. Calorimetry*, **105**, 157-160.

Yamaguchi, N. et al. (2015) Synthesis of CaO-SiO2 compounds using materials extracted from industrial waste. *Open J. Inorg. Non-Metallic Mater.*, **5**, 1-10.

Zapata, F. (2003) FAO/IAEA research activities on direct application of phosphate rocks for sustainable crop production. *In* Rajan, S. S. S. et al. (eds), Direct application of phosphate rock and related technology: Latest developments and practical experiences: Proceedings of an International Meeting, Kuala Lumpur, 16-20 July 2001, IFDC, Muscle Shoals, USA.

Zapata, F. & Roy, R. N. (2004) *Use of phosphate rocks for sustainable agriculture*. Food and Agricultural Organization of the United Nations, Rome.